JOURNAL OF Applied Polymer SCIENCE

Effect of cenosphere surface treatment and blending method on the tensile properties of thermoplastic matrix syntactic foams

B. R. Bharath Kumar,[1] Steven Eric Zeltmann,[2] Mrityunjay Doddamani,[1] Nikhil Gupta,[2] Uzma,[3] S. Gurupadu,[3] R. R. N. Sailaja[3]

[1]Lightweight Materials Laboratory, Department of Mechanical Engineering, National Institute of Technology Karnataka, Surathkal, Karnataka, India

[2]Composite Materials and Mechanics Laboratory, Mechanical and Aerospace Engineering Department, Tandon School of Engineering, New York University, Brooklyn, New York 11201

[3]Resource Efficient Process Technologies Application Division, The Energy and Resources Institute, Southern Regional Center, Bangalore 570 071, Karnataka, India

Correspondence to: M. Doddamani (E-mail: mrdoddamani@nitk.edu.in)

ABSTRACT: The influence of cenosphere surface treatment and blending method on the properties of injection molded high-density polyethylene (HDPE) matrix syntactic foams is investigated. Cenospheres are treated with silane and HDPE is functionalized with dibutyl maleate. Tensile test specimens are cast with 20, 40, and 60 wt % of cenospheres using injection molding. Modulus and strength are found to increase with increasing cenosphere content for composites with treated constituents. Highest modulus and strength were observed for 40 and 60 wt % untreated mechanically mixed and treated brabender mixed cenospheres/HDPE blends, respectively. These values are 37 and 17% higher than those for virgin and functionalized HDPE. Theoretical models are used to assess the effect of particle properties and interfacial bonding on modulus and strength of syntactic foams. Brabender mixing method provided highest ultimate tensile and fracture strengths, which is attributed to the effectiveness of Brabender in breaking particle clusters and generating the higher particle–matrix surface area compared to that by mechanical mixing method. Theoretical trends show clear benefits of improved particle–matrix interfacial bonding in the strength results. © 2016 Wiley Periodicals, Inc. J. Appl. Polym. Sci. **2016**, *133*, 43881.

KEYWORDS: composites; foams; mechanical properties; thermoplastics

Received 12 January 2016; accepted 29 April 2016
DOI: 10.1002/app.43881

INTRODUCTION

Excellent specific compressive strength and stiffness make hollow particle filled composites called syntactic foams promising candidates in lightweight structural applications.[1] Underwater vehicle structures, aircraft parts, thermoforming plugs, submarine buoyancy modules, and buoys are some of the notable applications for these materials.[2] Thermoset matrix syntactic foams having epoxy and vinyl ester matrices have been the focus of previous research. Although the challenges and feasibility of developing thermoplastic syntactic foams were first discussed over 45 years ago, the progress in these materials has been lacking.[3] Low- and high-density polyethylene (LDPE and HDPE), polylactic acid,[4] and polymethyl methacrylate (PMMA) are among the most widely used thermoplastic resins in consumer products, however, literature on thermoplastic matrix syntactic foams is scarce. An overview of thermoplastic matrix syntactic foams can be found in chapters of a recent book,[5,6] which also highlights the relative scarcity of literature for these material systems. Development of lightweight syntactic foams with higher mechanical properties than that of the matrix resin can help in weight saving in many existing applications of thermoplastic resins.

Fly ash is an industrial waste material generated in coal fired power plants and contains hollow particles called cenospheres.[7,8] Use of cenospheres as fillers can provide cost saving as well as weight saving. Cenospheres in fly ash primarily contain alumina and silica.[9] Environmental issues with fly ash disposal can be addressed by utilizing them in high performance thermoplastic syntactic foams.[10–12] Defects in the walls and non-sphericity compromise the properties of cenospheres compared to engineered hollow particles with perfect walls and spherical shape. Despite the presence of defects, the greater stiffness of their ceramic walls allow their properties to be in the range observed for the commonly used engineered glass microballoons.[13] To

Table I. Constituents Used for Developing Syntactic Foam Composites

Material	Grade	Role	Supplier
HDPE	HD50MA180	Matrix	Reliance Polymers, Mumbai, India
Cenosphere	CIL-150	Reinforcement	Cenosphere India, Kolkata, India
3-Amino propyl tri ethoxy silane (APTS)	—	Silane coating on cenospheres	Sigma–Aldrich, USA
Dibutyl maleate (DBM)	—	Functionalization of HDPE	S.D. Fine Chem, Mumbai, India.
Dicumyl peroxide	—	Initiator for compatibilization between silane coated cenosphere and functionalized HDPE	S.D. Fine Chem, Mumbai, India.

improve the interfacial bonding with different matrix resins, cenospheres have been treated with silane.[14] Improved interfacial bonding through functionalization of particles and thermoplastic resin leads to enhanced mechanical properties of syntactic foams.[15,16] Three-phase syntactic foams with HDPE matrix were studied with additional reinforcing phase of carbon nanotubes (CNT). Surface treatment of CNTs has also shown to improve the mechanical properties of these composites.[17] Functionalized HDPE has been used with untreated glass hollow particle fillers resulting in a noticeable increase in the tensile modulus and strength with no change to fracture toughness, compared to the same syntactic foam without compatibilizer.[18,19]

The present work is focused on synthesis of cenosphere/HDPE syntactic foams using an industrial scale plastic injection molding (PIM) machine to reduce the production time and cost. Optimization of injection molding temperature and pressure parameters was conducted in a previous work.[20] Using these optimized parameters, syntactic foams are fabricated using surface treated cenospheres and functionalized HDPE matrix. Cenospheres and matrix are mixed using two different blending routes to compare the effectiveness of these methods. The effect of each of these modifications on the tensile response of the syntactic foams is investigated in order to determine the optimal processing method.

EXPERIMENTAL

Materials

The materials used for fabricating syntactic foams are listed in Table I. The HDPE has a melt flow index of 20 g/10 min (190°C/2.16 kg). The resin is in granular form of 3-mm diameter and has a mean molecular weight of 97,500 g mol^{-1}. Cenosphere particle size and shape analysis is conducted using a Sympatec (Pennington, NJ) QICPIC high speed image analysis system.[21] Surface treatment of cenospheres and HDPE functionalization are performed according to the procedures described in earlier publications.[15,17,21] The cenospheres were analyzed by Fourier transform infrared (FTIR) spectroscopy to confirm the silane coating.[21] Functionalization of HDPE matrix resin is performed in a Brabender mixer (CMEI, MODEL-16 CME SPL, Western Company Keltron).

Sample Preparation

Two methods, mechanical mixing and Brabender mixing, are used in this work to mix HDPE matrix and cenospheres. Mechanical mixing is carried out manually resulting in no bonding between the constituents, whereas brabender mixing is carried out at 210°C.[15] Blend of cenosphere/HDPE from brabender in the form of small pellets having average mean diameter of 7 mm is seen in Figure 1. The mechanically- or Brabender-mixed blend of cenospheres with HDPE is fed into an industrial scale horizontal type single screw PIM machine (WINDSOR, 80 ton capacity). Tensile test samples are cast using PIM confirming to ASTM D 638-10 standard. Injection temperature and pressure are maintained at 160°C and 30 kg cm^{-2} as per the earlier optimization study.[20]

Table II lists the four types of syntactic foams fabricated in the present investigation. Specimens of each type are fabricated with 0, 20, 40, and 60 wt % cenospheres. The specimens are named according to the convention HXX-Y-ZZ, where H denotes the HDPE matrix, XX is the weight fraction of cenospheres, and Y-ZZ is the processing type name described in Table II. An overview of the different processing paths is presented in Figure 2. ASTM D792 – 13 standard was adopted to measure the density of all fabricated specimens. The densities of five specimens were measured and the average values and standard deviations are reported in Table III.

Tensile Testing

Tensile testing is conducted using a computer controlled universal test system (Z020 Zwick Roell, USA) with a 20 kN load cell. A constant crosshead displacement rate of 5 mm min^{-1} is maintained during the tests. Stress and strain are calculated from the acquired load and displacement data, respectively. Five

Figure 1. HDPE/cenosphere blend from brabender. [Color figure can be viewed in the online issue, which is available at wileyonlinelibrary.com.]

Table II. Syntactic Foam Types Fabricated in the Present Study

Specimen type	Cenospheres	HDPE	Mixing method
U-MM	Untreated	Virgin	Mechanical mixing
T_M-MM	Untreated	Functionalized	Mechanical mixing
T-MM	Silane treated	Functionalized	Mechanical mixing
T-BM	Silane treated	Functionalized	Brabender mixing

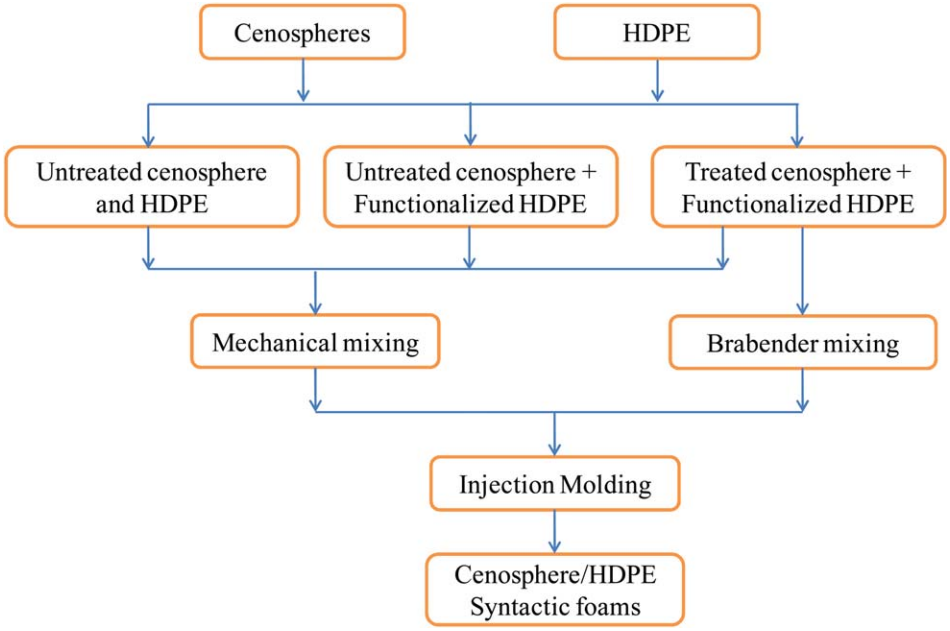

Figure 2. Fabrication routes and the types of cenosphere/HDPE syntactic foams synthesized in the present work. [Color figure can be viewed in the online issue, which is available at wileyonlinelibrary.com.]

specimens for each composite type are tested and average values are reported.

Imaging

Scanning electron microscopes (JSM 6380LA, JEOL, Japan and Hitachi S3400N, Tarrytown, NY) are used for microstructural analysis of as cast and fractured specimens. All the specimens are sputter coated prior to imaging (JEOL JFC-1600, Japan).

RESULTS AND DISCUSSION

Material Processing

Obtaining uniform dispersion of cenospheres and minimizing their crushing in the matrix is a challenging task, especially when using pressurized techniques like PIM. Figure 3(a) presents a representative micrograph of a syntactic foam containing untreated HDPE and cenospheres from a preliminary study on untreated constituents. Uniform dispersion of hollow cenospheres in the matrix is observed in this micrograph demonstrating the feasibility of using PIM for developing syntactic foam composites.[20] However, lack of interfacial bonding between cenospheres and HDPE is visible in Figure 3(b). Improvement in the cenosphere-HDPE interfacial bonding is desirable because tensile behavior strongly depends on the interfacial characteristics for effectively transferring load from the matrix to the particle. To promote strong interfacial bonding, cenospheres are treated with silane and HDPE is

Table III. Experimental Density Values of Syntactic Foams

Syntactic foam type	Experimental density (g cm^{-3})			
	U-MM	T_M-MM	T-MM	T-BM
H20	1.0159 ± 0.0016	1.0326 ± 0.0316	1.083 ± 0.0349	1.049 ± 0.0394
H40	1.0078 ± 0.0036	1.0293 ± 0.0414	1.111 ± 0.0455	1.071 ± 0.0434
H60	1.0219 ± 0.0071	1.0548 ± 0.0527	1.114 ± 0.0657	1.074 ± 0.0537

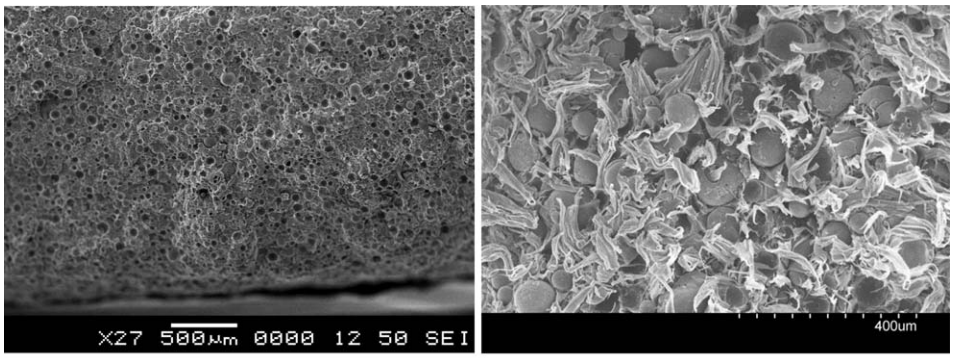

Figure 3. Micrograph of freeze fractured HDPE matrix syntactic foams containing 60 wt % cenospheres showing (a) uniform dispersion of cenospheres, indicating feasibility of using PIM in developing syntactic foams and (b) lack of bonding between cenospheres and HDPE matrix.

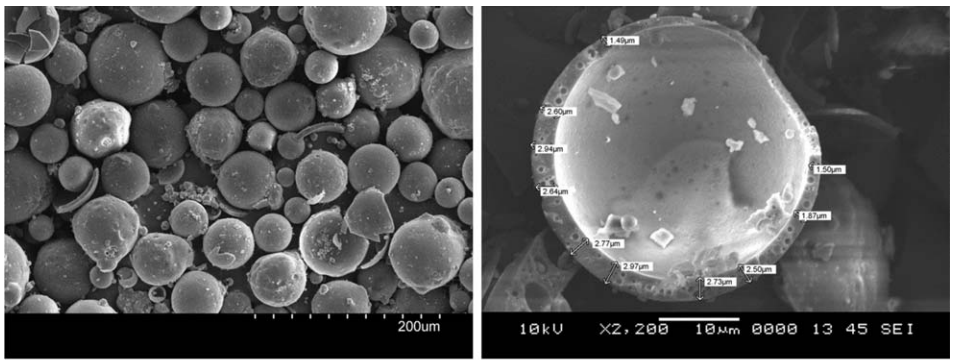

Figure 4. (a) Micrograph of as received cenospheres. (b) Surface imperfections, wall thickness variations within one particle and wall porosity can be observed in a broken cenosphere.

functionalized with 10 vol % DBM in the present study based on the existing literature.[15,21]

Cenospheres contain surface defects [Figure 4(a)], variation in wall thickness, and porosity in the particle walls [Figure 4(b)] leading to lower strength as compared to particles of fully dense walls of the same thickness. Particle size analysis for untreated and silane-treated cenospheres is presented in Figure 5. The volume-weighted mean particle size for untreated particles is 98 µm. The distribution for the coated particles is broader and shows a mean value of 109 µm. The tail of the distribution for treated particles indicates the formation of some clusters during the treatment process. The high shear forces generated during blending and injection molding are expected to break apart some of these clusters, though possibly at the expense of higher particle breakage. Particle sphericity is observed to be in the range of 0.6–0.85 from the particle size analysis, compared to 1 for perfectly spherical particles.[21]

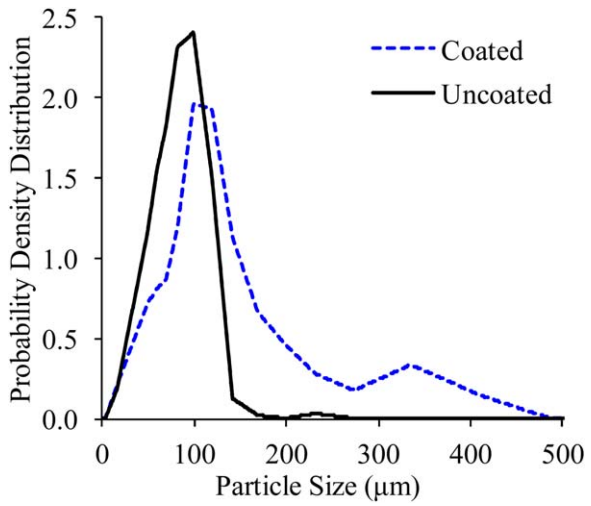

Figure 5. Particle size analysis of uncoated and silane treated cenospheres.[21] [Color figure can be viewed in the online issue, which is available at wileyonlinelibrary.com.]

A typical microstructure of syntactic foams with treated constituents is presented in Figure 6(a). The image is obtained on a freeze-fractured specimen. Cenospheres are uniformly dispersed in the functionalized HDPE resin as seen from this micrograph and clusters of particles are not present. A higher magnification micrograph in Figure 6(b) shows bonding between silane-treated cenospheres and the functionalized matrix, as evidenced by the presence of a continuous interface between them. Strong interfacial bonding is desired to enable effective transfer of load between the matrix and hollow particles to improve the tensile properties of syntactic foams.

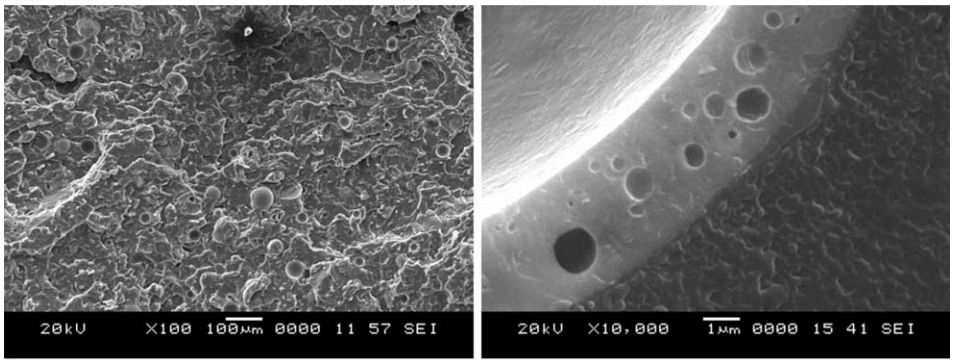

Figure 6. Micrographs of freeze fractured (a) treated cenosphere/HDPE syntactic foam showing uniform dispersion of 20 wt % cenospheres and (b) cenosphere–matrix interface. This specimen is processed by Brabender mixing followed by injection molding.

The difference between experimental and theoretical (calculated using rule of mixtures) densities is presented for all syntactic foams in Table III. Because no porosity is present in HDPE matrix, the difference between theoretical and experimental density values is attributed to the cenosphere breakage during manufacturing and is estimated by,

$$V_{mp} = \frac{\rho_t - \rho_m}{\rho_t} \quad (1)$$

where V_{mp}, ρ_t, and ρ_m are cenosphere porosity and theoretical and measured densities of syntactic foams. Negative porosity values indicate cenosphere breakage. During the syntactic foam synthesis using pressurized techniques like PIM, some cenospheres fracture. The matrix resin fills the cavity exposed due to cenosphere fracture, increasing the density of the syntactic foam. In the present case, experimental density is higher than the theoretical density values, implying particle breakage.

Stress–Strain Response

Virgin and Functionalized HDPE Resin. Figure 7 presents a representative set of stress–strain graphs for virgin and functionalized HDPE. Five specimens of each type are tested but only one specimen is shown to clearly illustrate the trends. Virgin HDPE exhibits failure strain of over 120% while the functionalized HDPE fails at 52% strain. With functionalization, failure strain reduces. The stress–strain graph for the virgin HDPE shows a long perfectly plastic region that ranges from 40 to 120% strain. A representative fractured specimen of virgin HDPE is presented in Figure 8(a). The long necking region in the HDPE specimen corresponds to the large plastic deformation as seen in the stress–strain graph. The inset in Figure 8(a) shows plastic deformation marks perpendicular to the direction of tensile loading throughout the specimen length. The final failure appears to be fibrous and has a broom-like fracture front, where plastic deformation seems to draw the fibers leading to fracture. The influence of functionalization on the failure pattern of HDPE specimens is evident in Figure 8(b), where the failure occurs at lower strain with only a little necking. In the virgin material, the polymer fibers act as separate entities [Figure 9(a)]. These micro-fibers stretch before breaking into a broom-like structure [Figure 8(a)], leading to higher failure strain. Functionalization changes the failure features at the microstructure level [Figure 9(b)]. Extensive localized plastic deformation followed by marks of elastic recovery is observed in the functionalized specimens due to crosslinking. It has been proposed that these changes following functionalization are likely related to the reduction in crystallinity and free volume

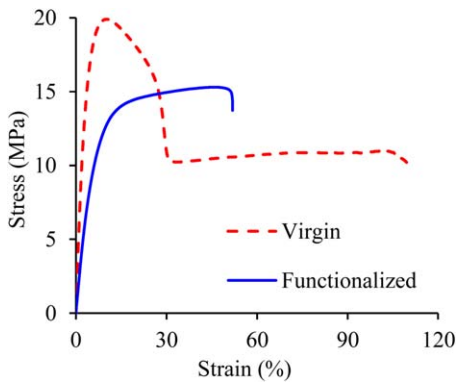

Figure 7. Comparison of representative stress–strain curves of virgin and functionalized HDPE. [Color figure can be viewed in the online issue, which is available at wileyonlinelibrary.com.]

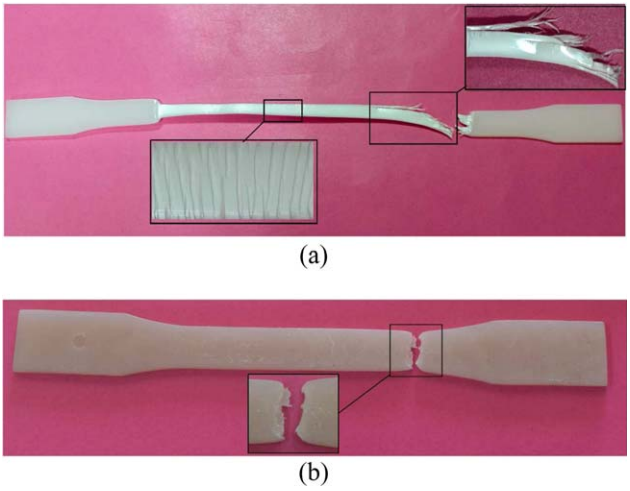

Figure 8. A representative failed specimen of (a) virgin[20] and (b) functionalized HDPE. [Color figure can be viewed in the online issue, which is available at wileyonlinelibrary.com.]

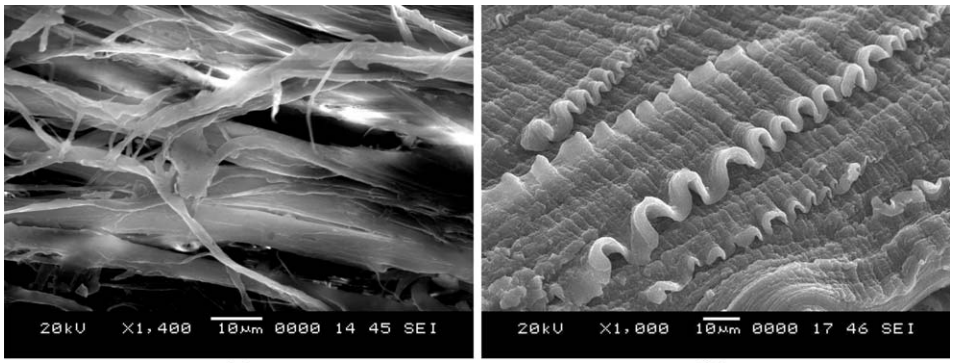

Figure 9. Micrographs of representative tensile tested specimen of (a) virgin and (b) functionalized HDPE.

Table IV. Tensile Properties of Virgin and Functionalized HDPE

HDPE	Modulus (MPa)	Elongation at UTS (%)	Fracture strain (%)	UTS (MPa)	Fracture strength (MPa)
Virgin	529 ± 19	10.21 ± 0.13	120.85 ± 6.86	19.9 ± 0.26	19.9 ± 0.19
Functionalized	228 ± 9	45.83 ± 1.12	51.91 ± 2.21	14.9 ± 0.19	15.3 ± 0.24

The values are presented in average ± standard deviation format.

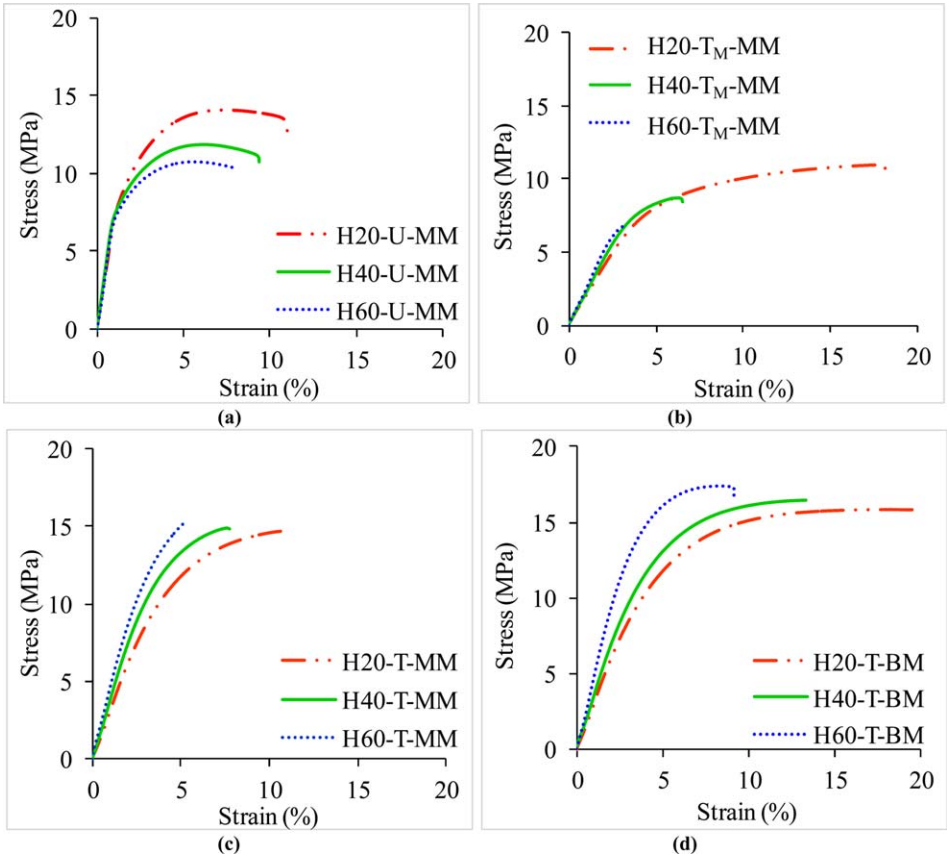

Figure 10. Stress-strain behavior of H20, H40, and H60 syntactic foams synthesized by (a) U-MM, (b) T_M-MM, (c) T-MM, and (d) T-BM routes. [Color figure can be viewed in the online issue, which is available at wileyonlinelibrary.com.]

Table V. Modulus, Elongation at UTS, and Fracture Strain of Syntactic Foams

Syntactic foam type	Modulus (MPa)				Elongation at UTS (%)				Fracture strain (%)			
	U-MM	T_M-MM	T-MM	T-BM	U-MM	T_M-MM	T-MM	T-BM	U-MM	T_M-MM	T-MM	T-BM
H20	574 ± 25	213 ± 8	268 ± 10	285 ± 12	7.42 ± 0.16	16.92 ± 0.19	10.86 ± 0.11	17.94 ± 0.44	10.38 ± 0.44	18.89 ± 0.55	11.02 ± 0.21	18.94 ± 1.11
H40	723 ± 33	226 ± 11	351 ± 14	327 ± 11	6.37 ± 0.34	6.25 ± 0.22	7.61 ± 0.28	12.82 ± 0.69	9.42 ± 0.72	7.09 ± 0.35	7.97 ± 0.33	13.29 ± 0.89
H60	661 ± 65	246 ± 17	375 ± 20	403 ± 19	5.61 ± 0.41	3.44 ± 0.34	3.13 ± 0.32	8.37 ± 0.51	7.76 ± 0.37	3.98 ± 0.83	5.34 ± 0.43	8.94 ± 0.63

Table VI. UTS and Fracture Strength of Syntactic Foams

Syntactic foam type	UTS (MPa)				Fracture strength (MPa)			
	U-MM	T_M-MM	T-MM	T-BM	U-MM	T_M-MM	T-MM	T-BM
H20	14.06 ± 0.10	10.92 ± 0.21	14.29 ± 0.55	15.86 ± 0.62	12.95 ± 0.38	10.39 ± 0.24	13.51 ± 0.31	15.37 ± 0.41
H40	12.07 ± 0.44	8.92 ± 0.39	14.81 ± 0.67	16.53 ± 0.51	11.18 ± 0.33	8.39 ± 0.31	14.21 ± 0.56	16.39 ± 0.71
H60	11.03 ± 0.55	7.33 ± 0.55	15.36 ± 0.79	17.44 ± 0.74	10.30 ± 0.55	6.73 ± 0.41	14.47 ± 0.71	16.45 ± 0.75

J. APPL. POLYM. SCI. 2016, DOI: 10.1002/APP.43881

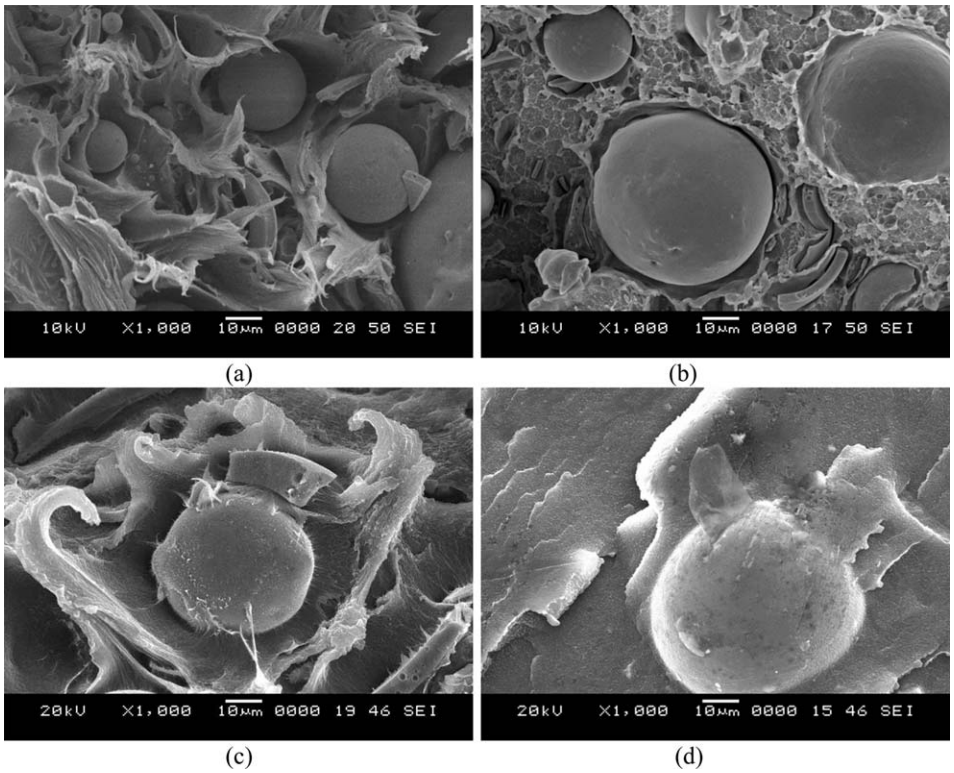

Figure 11. Micrographs of H40 syntactic foams synthesized by (a) U-MM, (b) T_M-MM, (c) T-MM, and (d) T-BM routes. All images are acquired at the same magnification.

caused by the presence of the maleate groups and their interactions with one another.[22,23]

The measured tensile modulus, ultimate tensile strength (UTS), elongation at UTS, and stress and strain at fracture of HDPE are listed in Table IV. The modulus, fracture strain, UTS, and fracture strength are of 132, 133, 34, 30% higher, respectively, for virgin HDPE compared to the functionalized polymer. However, for functionalized HDPE the elongation at UTS is 349% higher than for the virgin material.

Syntactic Foams. Representative stress–strain curves of syntactic foams prepared by different blending routes can be compared in Figure 10. The characteristics of the stress–strain curves are similar for all syntactic foam types with distinct elastic and plastic regions.

Tables V and VI present the tensile properties measured from these curves. The modulus of syntactic foams increases with cenosphere content except for H60-U-MM. This trend is very weak in the case of T-MM specimens [Figure 10(b)]. The addition of stiffer filler particles that are strongly bonded to the matrix restricts the mobility of the matrix, increasing the modulus. Due of the relatively lower filler content, H20 samples show the highest strain at UTS and fracture strain among all syntactic foams for all processing paths. Functionalization of the HDPE leads to a decrease in the modulus of the matrix, which is only partially compensated by the modulus gains resulting from improved interfacial bonding of the cenospheres. The behavior of syntactic foams is also dependent on particle survival during processing. Because only the outer surface of the particles is coated with the coupling agent, the fragments of broken particles cannot bear load as effectively as the intact particles. Among the treated composites, the greatest increase in modulus is observed for T-BM processing. Improved cenospheres–HDPE dispersion and interfacial bonding owing to reactive blending in the Brabender results in this trend. Elongation at UTS and fracture strain decreases with increase in filler content for all the blending routes. The presence of the stiff filler particles restricts the ability of the matrix to flow and form stable fibers as observed in the failure surfaces of virgin HDPE. For the syntactic foams with treated constituents, elongation at UTS decreases in the range of 116–397% whereas this reduction for U-MM is merely 32% with respect to lowest filler content. The syntactic foams also fracture at significantly lower strain compared to the neat HDPE specimens. Fracture strain reduces by 34% in U-MM, while a decrease of 112–375% was seen with treated constituents with respect to the neat resin. The lack of necking and large-scale plastic deformation is apparent in the stress–strain graphs of the syntactic foams.

It can be observed from Figure 10(b–d) and Table VI that the strength of syntactic foams decreases for U-MM, T_M-MM and increases in case of T-MM and T-BM, with increasing cenosphere content. Micrographs of representative H40 specimens acquired for all the blending routes are presented in Figure 11. Cenospheres-HDPE bonding is poor in U-MM mixing as observed by Figure 11(a). Further, though HDPE is functionalized, an absence of interfacial bonding in T_M-MM is observed due to untreated cenospheres in Figure 11(b). Figure 11(c) shows linkages between cenospheres and HDPE resulting in

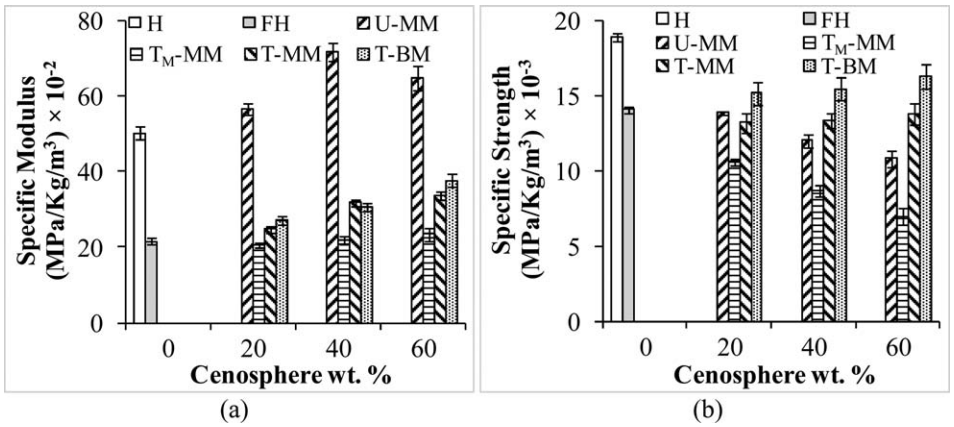

Figure 12. (a) Specific modulus and (b) specific strength of all samples with investigated blending routes.

improved interfacial strength in T-MM, which improves UTS and fracture strength in these syntactic foams compared to U-MM and T_M-MM specimens. Finally, reactive blending in T-BM forms a seamless interface between the filler and matrix as evident from Figure 11(d), resulting in the highest strength levels. It can also be noted in Table VI that the UTS decreases with increasing cenosphere content for U-MM and T_M-MM, while a reverse trend is observed for T-MM and T-BM syntactic foams. Decrease in the load bearing section due to lower matrix content at higher filler loading results in a reduction of UTS in the specimens when the interfacial bonding is poor. Functionalization of HDPE promotes effective load transfer through the particle–matrix interface, which is evident in the higher UTS and fracture strengths. While improvement in the interfacial bonding has improved the properties of syntactic foams, the decision to use these treatment methods must weigh the property benefits against increased processing time, costs, and the environmental impacts in the context of the proposed application of syntactic foams.

Further, specific modulus for U-MM is higher compared to all other configurations (Figure 12). Higher particle survival in U-MM results in higher modulus with retained porosity leads to higher specific modulus. Specific strength decreases with increase in filler content while seen to be increasing for treated configurations. At 20% filler loading, specific strength or U-MM is comparable with T-BM with marginal difference at 40%. H40-U-MM seems to be an optimal choice from both modulus and strength point of view.

Theoretical Modeling

To better understand the effects of the processing parameters on the properties of syntactic foams, theoretical modeling approaches are applied to the experimental results. The existing models relate the elastic properties of syntactic foams to the elastic modulus of matrix and particle and the particle wall thickness.[24–26] The particle wall thickness is modeled in the form of a parameter called radius ratio η, which is defined as the ratio of inner to the outer radius of the hollow particles.[26,28] The radius ratio $\eta = 1$ corresponds to an air void and $\eta = 0$ corresponds to a solid particle. In tensile loading, the effect of these parameters on the ultimate strength is dominated by the effects of particle-matrix debonding in low stiffness polymer matrices. Therefore, the tensile strength of syntactic foams can often be modeled effectively using general solid particulate composite approaches with appropriate effective stiffness of

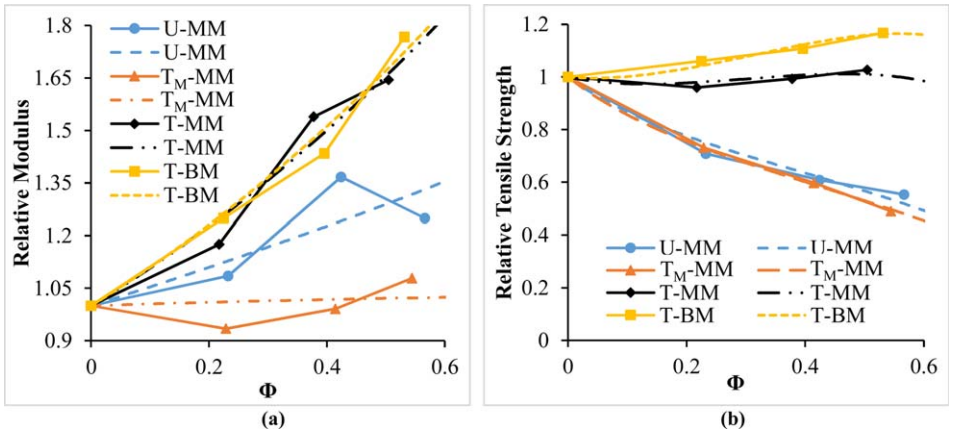

Figure 13. Least squares best fits of (a) Bardella–Genna model for modulus and (b) Pukánszky model for tensile strength represented with respect to the properties of neat resin. Solid lines with symbols represent experimental data and dashed lines are model fits. [Color figure can be viewed in the online issue, which is available at wileyonlinelibrary.com.]

particles, without considering the geometric effect of wall thickness or void. In this work, the tensile modulus is modeled using the Bardella–Genna model for syntactic foams[25] and the tensile strength is modeled using the Pukánszky model modified for hollow particles.[29] For both models, the volume fraction of hollow particles Φ in syntactic foams is calculated from the nominal mass fraction and is reduced according to the estimated particle breakage fraction obtained from density measurements of the fabricated specimens, considering that there is no entrapped air porosity in the matrix.

Tensile Modulus. The theoretical models for hollow particle composites, including the Bardella–Genna model used here, assume that there is perfect bonding between the particle and the matrix. An approach is taken where the model is used to obtain a least squares best fit estimate of the radius ratio parameter η, while using the wall material modulus that is calculated according to the cenosphere composition. This effective value for η encapsulates information about the loss in reinforcing capability of cenospheres due to defects in the particle wall as well as due to the imperfect interfacial bonding. The rule of mixtures approach for determining the properties of the ceramic wall is described in a previous work[20] and yields the elastic modulus and Poisson's ratio of 157.4 and 0.185 GPa, respectively. Using these parameters, the measured modulus of the matrix, and assuming the Poisson's ratio of HDPE to be 0.425, the model is fitted to the experimental data for each material type with the radius ratio as the free parameter. The full expression of this micromechanics-based model is lengthy and the reader is directed to the original article.[25] The resulting model predictions are compared to the experimental data in Figure 13(a). For U-MM, T_M-MM, T-MM, and T-BM the effective radius ratios are found to be 0.9945, 0.9986, 0.9957, and 0.9956, respectively. These values are significantly higher than that obtained by density measurements and measurement in SEM images, which yield a radius ratio around 0.9,[21] indicating that for all the syntactic foams the stiffening efficiency of the particles is significantly lower than what is expected for particles of defect free walls having perfect bonding with the matrix. Testing in compression would likely yield a smaller effective radius ratio (greater stiffening effect) because the matrix is pushed onto the interface reducing the importance of interfacial bonding. T-MM and T-BM have approximately the same effective cenosphere properties, and T_M-MM shows the lowest effective properties (highest effective η). U-MM shows the lowest effective η of all the compositions because the higher matrix modulus leads to a lower particle wall to matrix modulus ratio, which the model compensates for by increasing the effective wall thickness.

Tensile Strength. The models for the tensile strength of particulate-reinforced composites are strictly decreasing functions with filler volume fraction[30] as it is generally assumed that matrix is the main load bearing phase and poor interfacial adhesion prevents effective load transfer from the matrix to the particle. For composites that do not necessarily follow this trend, the relationship proposed by Pukánszky *et al.*[29,31] can be applied. The model is expressed as

$$\sigma_c = \frac{1-\Phi}{1+2.5\Phi}\sigma_m \exp(B\Phi) \quad (2)$$

where σ_c is the strength of the composite, σ_m is the strength of the matrix, and the parameter B is related to the interfacial strength. There is no reinforcing effect when $B = 0$, while the strength of the composite increases with increasing filler content for $B > 3$. For U-MM and T_M-MM the value of B is $\sim$1.81, while for the two types of syntactic foams with strong interfacial bonding, T-MM and T-BM, the value of B is found to be about 3.17. These results show that syntactic foams with untreated particles have poor interfacial bonding and the strength decreases with particle content and provide quantitative insight into the improvement caused by the particle surface and matrix modification. Treatment of the particles has a significant impact on the interfacial bonding, causing the strength to increase with particle content.

CONCLUSIONS

The effect of surface treatment and blending method on the tensile behavior of cenosphere/HDPE syntactic foams produced by an industrial scale injection molding technique is studied in the present work. Use of fly ash cenospheres in composites can make them lighter, reduce the consumption of HDPE and address the environmental concern of fly ash disposal. The main conclusions can be summarized as:

- The surface treatment of cenospheres and functionalization of HDPE promote interfacial bonding resulting in most property improvement.
- Tensile modulus of syntactic foams was found to increase with cenosphere content except for U-MM, which used untreated particles and matrix resin.
- Strength increases with cenosphere content when both treated HDPE and cenospheres are used, and decreases otherwise.
- The modulus and strength are found to be the highest for H40-U-MM (723 MPa) and H60-T-BM (17.4 MPa) specimens. These values are 37 and 17% higher than those for their respective matrices.
- While surface treatment yields benefits in the reinforcing capabilities of cenospheres, the use of untreated constituents (U-MM) may still be beneficial where modulus is an important criterion, rather than the strength.

ACKNOWLEDGMENTS

Authors acknowledge Dr. Keshav Prabhu, Mr. Puneeth, and Mr. Praveen of Konkan Speciality Polyproducts Pvt. Ltd., Mangalore, Karnataka, India for providing the Injection molding facility for casting the samples and useful discussions. Acknowledgement is also due to Director, TERI, for providing Brabender facility for preparing the blends. Author Nikhil Gupta acknowledges the Office of Naval Research grant N00014-10-1-0988. The views expressed in this article are those of authors, not of funding agencies. The authors thank the ME Department at NIT-K and MAE Department at NYU for providing facilities and support.

REFERENCES

1. Gupta, N.; Zeltmann, S.; Shunmugasamy, V.; Pinisetty, D. *Jom* **2014**, *66*, 245.
2. Gupta, N.; Pinisetty, D.; Shunmugasamy, V. C. Reinforced Polymer Matrix Syntactic Foams: Effect of Nano and Micro-Scale Reinforcement. Springe Briefs in Materials; Springer International Publishing, New York, **2013**.
3. Waite, W. A.; Waldron, M. L.; Nahabedian, A. *Naval Eng. J.* **1969**, *81*, 95.
4. Bachmatiuk, A.; Börrnert, F.; Schäffel, F.; Zaka, M.; Martynkowa, G. S.; Placha, D.; Schönfelder, R.; Costa, P. M. F. J.; Ioannides, N.; Warner, J. H.; Klingeler, R.; Büchner, B.; Rümmeli, M. H. *Carbon* **2010**, *48*, 3175.
5. Yalcin, B. In Hollow Glass Microspheres for Plastics, Elastomers, and Adhesives Compounds; Amos, S. E., Yalcin, B. Ed.; William Andrew Publishing (Elsevier): Oxford, **2015**; p 175.
6. Yalcin, B.; Amos, S. E. In Hollow Glass Microspheres for Plastics, Elastomers, and Adhesives Compounds; Amos, S. E., Yalcin, B., Eds.; William Andrew Publishing (Elsevier): Oxford, **2015**; p 35.
7. Li, J.; Agarwal, A.; Iveson, S. M.; Kiani, A.; Dickinson, J.; Zhou, J.; Galvin, K. P. *Fuel Process. Technol.* **2014**, *123*, 127.
8. Lauf, R. J. *Fuel* **1981**, *60*, 1177.
9. Anshits, N. N.; Mikhailova, O. A.; Salanov, A. N.; Anshits, A. G. *Fuel* **2010**, *89*, 1849.
10. Gupta, N.; Singh Brar, B.; Woldesenbet, E. *Bull. Mater. Sci.* **2001**, *24*, 219.
11. Satapathy, B.; Das, A.; Patnaik, A. *J. Mater. Sci.* **2011**, *46*, 1963.
12. Qiao, J.; Wu, G. *J. Mater. Sci.* **2011**, *46*, 3935.
13. Doddamani, M.; Kishore, V. C.; Shunmugasamy, N.; Gupta, H.; Vijayakumar, B. *Polym. Compos.* **2015**, *36*, 685.
14. Wang, W.; Li, Q.; Wang, B.; Xu, X. T.; Zhai, J. P. *Mater. Chem. Phys.* **2012**, *135*, 1077.
15. Deepthi, M. V.; Sharma, M.; Sailaja, R. R. N.; Anantha, P.; Sampathkumaran, P.; Seetharamu, S. *Mater. Des.* **2010**, *31*, 2051.
16. Chand, N.; Sharma, P.; Fahim, M. *Mater. Sci. Eng. A* **2010**, *527*, 5873.
17. Divya, V. C.; Ameen Khan, M.; Nageshwar Rao, B.; Sailaja, R. R. N. *Mater. Des.* **2015**, *65*, 377.
18. Patankar, S. N.; Das, A.; Kranov, Y. A. *Compos. A* **2009**, *40*, 897.
19. Patankar, S. N.; Kranov, Y. A. *Mater. Sci. Eng. A* **2010**, *527*, 1361.
20. Bharath Kumar, B. R.; Doddamani, M.; Zeltmann, S. E.; Gupta, N.; Ramesh, M. R.; Ramakrishna, S. *Mater. Des.* **2016**, *92*, 414.
21. Bharath Kumar, B. R.; Doddamani, M.; Zeltmann, S. E.; Gupta, N.; Uzma, U.; Gurupadu, S.; Sailaja, R. R. N. *J. Mater. Sci.* **2016**, *51*, 3793.
22. Wang, Y.; Ji, D.; Yang, C.; Zhang, H.; Qin, C.; Huang, B. *J. Appl. Polym. Sci.*. **1994**, *52*, 1411.
23. Girija, B. G.; Sailaja, R. R. N. *J. Appl. Polym. Sci.* **2006**, *101*, 1109.
24. Bardella, L.; Sfreddo, A.; Ventura, C.; Porfiri, M.; Gupta, N. *Mech. Mater.* **2012**, *50*, 53.
25. Bardella, L.; Genna, F. *Int. J. Solids Struct.* **2001**, *38*, 7235.
26. Porfiri, M.; Gupta, N. *Compos. B Eng.* **2009**, *40*, 166.
27. Gupta, N.; Woldesenbet, E.; Mensah, P. *Compos. A: Appl. Sci. Manufact.* **2004**, *35*, 103.
28. Gupta, N.; Woldesenbet, E. *J. Cell. Plast.* **2004**, *40*, 461.
29. Turcsányi, B.; Pukánszky, B.; Tüdõs, F. *J. Mater. Sci. Lett.* **1988**, *7*, 160.
30. Fu, S. Y.; Feng, X. Q.; Lauke, B.; Mai, Y. W. *Compos. B Eng.* **2008**, *39*, 933.
31. Pukánszky, B. *Composites* **1990**, *21*, 255.